Passive Stall Control Systems of Power Limitation Modes for Vertical Axis Wind Turbines (VAWT)

Ihor Shchur, Andrii Lozinskyi, Bohdan Kopchak, Yurii Biletskyi and Vsevolod Shchur

Abstract Vertical axis wind turbines (VAWT) with direct drive permanent magnet synchronous generator operate with the greatest energy efficiency and reliability in low-power wind energy conversion systems (WECS). This article offers a classification of optimal control methods of such WECS. Special attention is also given to an unexplored area—the development of control systems of power limitation mode when VAWT work at high wind speeds—passive stall and feathering control. In particular, the structures of control systems were developed, the parameters of power regulators were obtained, and these regimes were compared by means of computer simulation. The fractional order control method was also used for this mode and the parameters of fractional order PID power regulator were found by the method of Particle Swarm Optimization (PSO). The article also demonstrates how to realize the mode of passive stall control in the energy-shaping control system (ESCS) previously developed by the authors.

Keywords VAWT · PMSG · Optimum control · Power limitation modes · Passive stall regulation · Fractional order control · Energy-shaping control

I. Shchur (✉) · A. Lozinskyi · B. Kopchak · Y. Biletskyi · V. Shchur
National University „Lviv Polytechnic“, Lviv, Ukraine
e-mail: i_shchur@meta.ua

A. Lozinskyi
e-mail: addriy.o.lozynskyy@lpnu.ua

B. Kopchak
e-mail: kopchakb@gmail.com

Y. Biletskyi
e-mail: shadovv00@gmail.com

V. Shchur
e-mail: lesyk_shchur@yahoo.com

D. Mazur et al. (eds.), *Analysis and Simulation of Electrical and Computer Systems*, Lecture Notes in Electrical Engineering 452,
https://doi.org/10.1007/978-3-319-63949-9_8

1 Introduction

In many countries, especially in highly developed countries, the rate of renewable energy is increasing. Prominent in this process is the wind energy that is represented by high power wind turbines (WT) with the horizontal axis of rotation (HAWT), which are often combined in wind farms [1]. Along with this, low-power (up to 10 kW) wind energy conversion systems (WECS) recently are becoming more and more common [2]. They are used by individual consumers for power supply in case of lack of centralized power grids, or if the availability of the latter for additional power supply to reduce power consumption from the grid, increase energy efficiency, ensuring uninterrupted power supply, etc. [3]. Specific work conditions of low-power WECS cause significant differences from powerful HAWT in design and tasks of automatic control of their work in different modes.

Low-power WECS are installed directly at consumers, where the wind is mostly characterized by low average speeds, frequent gusts, changes in direction and high turbulence. Features of location and specific characteristics of wind determine the benefits of the application of WT with a vertical axis of rotation (VAWT). These turbines operate efficiently with gusty winds, constantly perceive the wind from any directions, and start at low wind speeds thanks to low-speed gearless drive of the multipolar synchronous generator with permanent magnets (PMSG) [4]. The vertical design of VAWT makes it possible to place a relatively large PMSG under WT, which will not affect the aerodynamic characteristics of the latter. The absence of mechanical multiplicator reduces the starting wind speed of VAWT.

Unlike HAWT, which is based on the traditional pattern and differ mainly in the number of blades, in VAWT there is a huge variety, which due to the current elevated interest in wind power is growing. VAWT may differ by the following features: prevailing principle of operation (the drag or lift) and accordingly the value of tip speed ratio (TSR); passive or active design (rigidly mounted or rotary blades); the number of WT working on a generator; using power augmentation-guide-vane and more [5].

The specific (on a unit of power) cost of low-power VAWT is much higher than powerful HAWT. Therefore, to reduce the payback period, the low-power WECS must produce maximum energy efficiency in all modes of operation, especially at low wind speeds, because in these conditions these WT are the vast majority of the time. The practice of VAWT application allows selecting the most efficient configuration. Thus, the WT of passive construction have the lowest cost and highest reliability. The straight-blade VAWT (SB-VAWT) with corresponding aerodynamic profile NACA excel by the highest power density due to high TSR and low cost [6]. However, lack of opportunity to adjust the aerodynamic characteristics of passive VAWT leaves you to make automatic control of WECS only by changing of generator electrical load. To this end, there are two most commonly used configurations of power electronic control systems, with cheaper passive diode rectifier DB and DC/DC converter and more expensive with a voltage active rectifier (AR) (Fig. 1) [7]. As loading in both systems used the battery B, which is

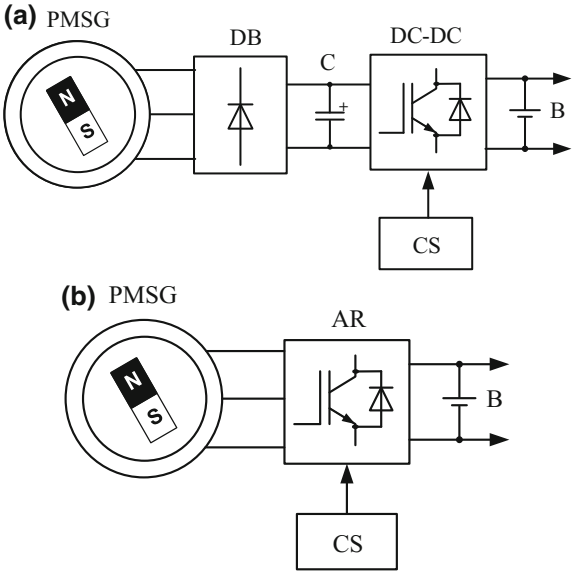

Fig. 1 Common controlled electromechanical systems for WECS with VAWT and PMSG: **a** based on a DC/DC converter, **b** based on an AR

connected to the electrical consumers via direct current or through voltage inverter —AC. Apart from cost, these systems differ also a number of other indicators, but allow you to provide the desired load regulation of PMSG, so a type of electronic system is not essential for the building of control system. Automatic control of these WECS made respective control systems CS.

Much more energy efficiency and safety of WECS with VAWT depends on the approaches to the design of control systems and therefore the quality of their work.

The main objective of this paper is to analyze approaches to creating automatic control systems (ACS) for WECS with VAWT and research of control systems for power limitation of passive VAWT at its work on the winds at a speed higher than the nominal.

The paper is organized as follows: Sect. 2, under the basic laws of VAWT operation, introduces the classification of control systems of optimal loading of PMSG in partial-load operating mode and shows how VAWT power can be limited in the full-load operating mode when wind speed is higher than the nominal. Section 3 is devoted to the creation and research by computer simulation of systems to VAWT power limitation using classic controllers. Section 4 shows how you can improve the system power limitation using fractional order PID power regulator. In Sect. 5 we researched and developed the subsystem of VAWT power limitation for developed previously by the authors the energy-shaping control system (ESCS), designed for optimal control of WECS describing as a port-controlled Hamiltonian system (PCHs). Finally, some conclusions are discussed.

2 The Main Patterns of VAWT Work in Different Modes and Control Systems Review

At any moment WECS is at a certain operating point, which depends on a number of factors: wind speed V, the angular velocity ω of VAWT, the power of electrical loads of PMSG, the efficiency of the generator at this point, the nature of work (transient or steady state mode).

The output power of the VAWT shaft, which creates by wind flow, described by the known expression

$$P_{\mathrm{WT}} = \frac{1}{2}\rho A C_{\mathrm{P}}(\lambda) V^3, \tag{1}$$

where ρ is the air density, $A = 2\,r\,h$ is the washing area of SB-VAWT with the radius r and the height of blade h, C_{P} is the power coefficient, and $\lambda = \omega\, r/V$ is the TSR.

Power coefficient function $C_{\mathrm{P}}(\lambda)$ is the main dimensionless characteristic of the VAWT aerodynamic properties, which is generally considered to be stable (for aerodynamically passive VAWT) and independent of WT working conditions [8].

The mechanical torque on the VAWT shaft is equal

$$T_{\mathrm{WT}} = \frac{P_{\mathrm{WT}}}{\omega} = \frac{1}{2}\rho\, A\, r \frac{C_{\mathrm{P}}(\lambda)}{\lambda} V^2. \tag{2}$$

According to expressions (1) and (2), power coefficient function $C_{\mathrm{P}}(\lambda)$ determines the nature of power and torque of the VAWT. These characteristics for specific WT can be obtained by calculation or by modeling of aerodynamic processes during WT work by finite element method in CFD (Computation Fluid Dynamics) [9], or experimentally in wind tunnels. In further studies we will use the dependence, which is typical for 3-blads low-power SB-VAWT (Fig. 2):

$$C_{\mathrm{P}}(\lambda) = 1.14\left(\frac{9.47}{\lambda} - 1\right)\mathrm{e}^{\frac{-6}{\lambda}}. \tag{3}$$

Dependence $C_{\mathrm{P}}(\lambda)$, as shown in Fig. 2, provides the maximum value of power coefficient $C_{\mathrm{P\,max}} = 0.3514$ for the optimal value of TSR $\lambda_{\mathrm{opt}} = 3.675$. The point $C_{\mathrm{P\,max}}(\lambda_{\mathrm{opt}})$ is called maximum power point (MPP). To support the work of VAWT at this point, its angular velocity must be maintained at an optimum value, which should be directly proportional to the wind speed:

$$\omega_{\mathrm{opt}} = \frac{\lambda_{\mathrm{opt}}}{r} V. \tag{4}$$

Based on $C_{\mathrm{P}}(\lambda)$, from (1) and (2) basic dependences can be calculated for particular VAWT, which characterize its work. Figures 3 and 4 show the calculated

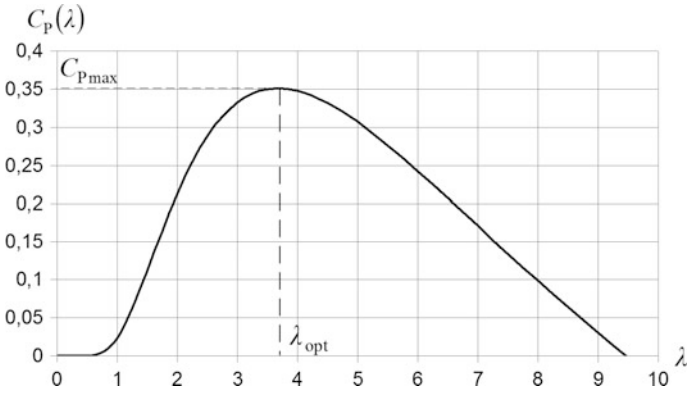

Fig. 2 Power coefficient function of SB-VAWT adopted in this paper

curves, respectively, torque and mechanical power on a shaft of VAWT vs its angular velocity at constant values of wind speed for WT with aerodynamic characteristic (3) and the rated power of 1 kW, which obtains at the wind speed of 10 m/s. The curve of VAWT optimal torque values T_{opt}, shown in Fig. 3, corresponds to the curve of maximum power P_{max}, connecting the extremes of the curves in Fig. 4.

One of the most important characteristics of WECT is its power curve—a dependence of output electrical power P_{WECS} versus wind speed. Functions of this type (Fig. 5) usually are served graphically in passports of specific WECS by manufacturers [10].

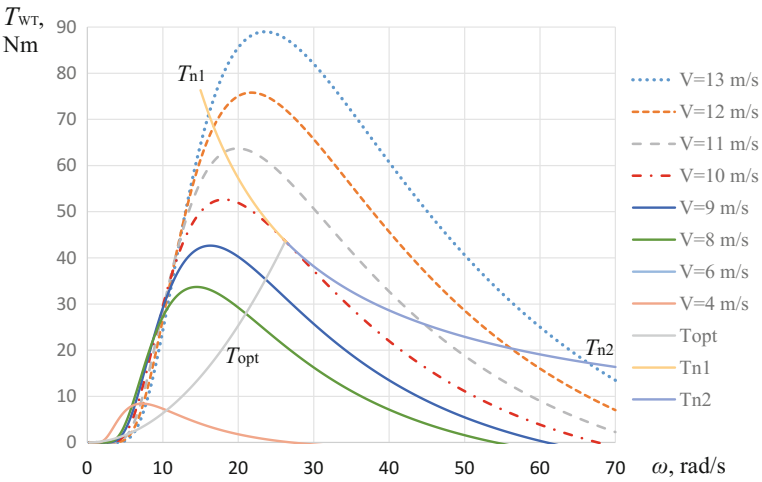

Fig. 3 Mechanical torque on the VAWT shaft versus its angular velocity for WT with rated power of 1 kW at different wind speeds

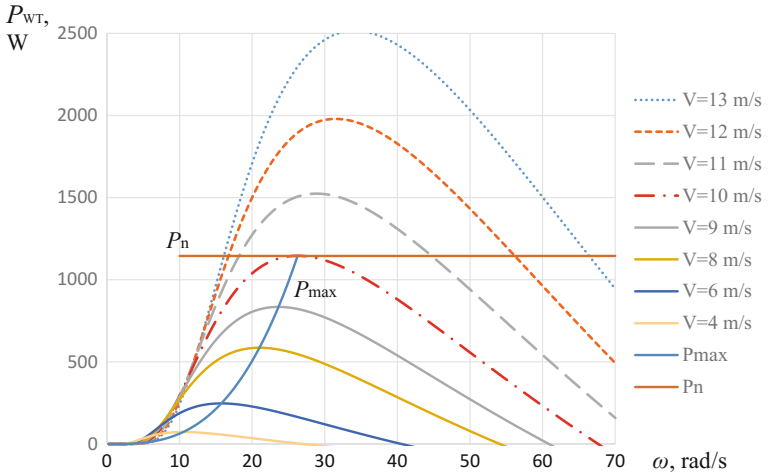

Fig. 4 Output mechanical power on the VAWT shaft vs its angular velocity for WT with rated power of 1 kW at different wind speeds

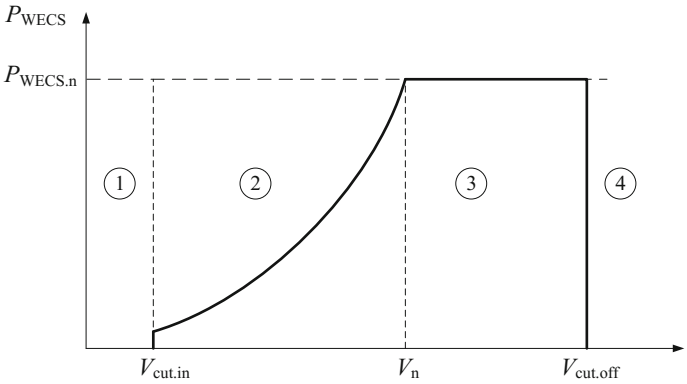

Fig. 5 Typical power curve of WECS

Figure 5 highlight 4 zones. WT will not start in zone 1 because of the low wind speed and starts generating the output electricity from the wind speed $V_{cut.in}$, known as the cutting speed and, usually between 3 and 4 m/s. In the range of wind speeds from $V_{cut.in}$ to the rated wind speed V_n (control zone 2) WT work with partial-load, and only at wind speed, V_n output power of WT reaches its nominal value $P_{WECS.n}$, for which an electric generator is designed. In the range of wind speed from V_n to $V_{cut.off}$, called cutting speed, (control zone 3) the electric output power of WT must be limited at rated level by one of the possible ways. With increasing of wind speed over $V_{cut.off}$ braking system works, VAWT ceases to rotate, and therefore process of generating electricity stops (zone 4).

The most task of automatic control of WECT with aerodynamically passive VAWT (fixed blades) with partial-power at low and average wind speeds is ensuring optimal electrical load of PMSG that VAWT always moved with optimum proportional to wind speed angular velocity according to (4) and worked in MPP—Maximum Power Point Tracking (MPPT) [11]. Substituting in (2) the value of the wind speed from Eq. (4), we obtain the following relationship:

$$T_{\text{opt}} = \frac{0.5\rho A C_{\text{P max}} r^3}{\lambda_{\text{opt}}^3} \omega_{\text{opt}}^2 = K_{\text{T}} \omega_{\text{opt}}^2, \tag{5}$$

where $K_{\text{T}} = \frac{0.5\rho r^3 A C_{\text{P max}}}{\lambda_{\text{opt}}^3}$.

The law on the formation of the reference mechanical torque $T_{\text{WT}}^* = K_{\text{T}} \omega^2$ by the mean of PMSG load is the most common for optimal sensorless control providing asymptotic movement of VAWT operating point to the MPP.

Maximum output power of VAWT is not a goal in contrast to the power of electricity at WECT output. That value depends also on the loss of a channel, power transformation, and transmission. Therefore, the goal of optimal control at the site of partial-power WT must be the maximum approaching power curve in static and dynamic modes (Fig. 5), which is applied in several studies [12, 13].

In the partial-load operating mode (control zone 2) WECT is an overwhelming amount of time, thus generating electricity from small power. The extremely high requirements to quality of control systems work, providing optimal control in order to obtain maximum power from the wind. Based on the analysis of scientific publications on this subject we identified the following classification criteria of optimal control systems for WECS with VAWT:

(a) type of control—passive [14], active [15], active–passive [16];
(b) availability of wind speed sensors—sensors and sensorless [11, 15];
(c) availability of information about the performance of the components of WECS—VAWT (characteristic $C_{\text{P}}(\lambda)$, the point of maximum power $C_{\text{Pmax}}(\lambda_{\text{opt}})$, optimal TSR λ_{opt}), generator (the dependence of efficiency from power and angular velocity), whole WECS (power curve $P_{\text{WECS}}(V)$), without the need of any data [11, 15];
(d) principle of automatic control—as to disturbance (optimal torque control—OTC) [11], as to deviation (TSR-control, optimal power control—OPC) [11], intelligent (fuzzy-logic control—FLC, artificial neural network—ANN) [17, 18], search control (perturbation and observation—P&O, hill-climb searching—HCS) [11, 19, 20];
(e) mathematical description and corresponding methods of control—linearized [11], nonlinear (adaptive control [21], sliding mode control—SMC [22], feedback linearization control [23]), control based on energy approach (passive-based control—PBC, energy-shaping control—ESC) [24].

The task of automatic control of WECS operation in large wind speeds (zone 3 in Fig. 5) is to limit the electrical power output at rated value, especially for PMSG

that eliminates overheating. Limitations are also associated with acceptable mechanical loads on VAWT. In powerful HAWT for this purpose active pitch-control unfolding blades are used for their interaction with a smaller airflow [8]. In some low-power VAWT also, pitch-controlled blades or special additional plates that rise on high VAWT angular velocity are used and create additional aerodynamic resistance [18]. However, it significantly complicates WECS and reduces the reliability of its work in adverse weather conditions.

In WECS with SB-VAWT, we can achieve a similar effect by the special control system, which, through appropriate regulation of generator load speed and, respectively, VAWT angular velocity, shifts the operating point of VAWT so that it captured less power from wind flow. Herewith, there are two areas of regulation, which correspond to two flat parts of the curve $C_P(\lambda)$ (Fig. 2), which lie on opposite sides of λ_{opt}. If at increasing of wind speed the angular velocity of VAWT decreases, the λ decline, reducing the value of power coefficient CP. This is so-called passive stall regulation [25]. With appropriate work of control system, we can stabilize VAWT power by reducing its angular velocity and increasing mechanical torque. If at increasing of wind speed VAWT rotates at a much higher angular velocity so that it substantially exceeded λ_{opt}, it is also possible to stabilize power, but on the contrary—by reducing the mechanical torque of VAWT. This mode is called feathering regulation [25].

If we limit the power of research VAWT at the rated level $P_{WT.n}$ = 1145 W, as shown in Fig. 4, that for this power get the dependences of VAWT torque from its angular velocity in the areas of stall regulation T_{n1} and feathering regulation T_{n2} (Fig. 3). As seen in the last, in the area of stall regulation the VAWT torque considerably increases, which should be provided in its design. According to the torque and the current of PMSG increase too that causes additional losses in the armature winding of the generator. In the area of feathering regulation, rather—the torque and the loss of copper in the generator decrease, but significantly increase the angular velocity of VAWT and generator, which also must be provided in the construction of WECS.

Unfortunately, passive stall and feathering regulation do not find proper coverage in special scientific literature. Automatic control mode that provides passive stall regulation of VAWT devoted some attention in papers [26, 27].

Control of small VAWT in the work [26] carried out by adjusting the DC voltage U_{DC} in the output of diode bridge, by which PMSG is loaded. In electrical power limiting mode, the fast PI controller comes into work. It reduces the reference on U_{DC}, which, in turn, is regulated in a closed system by varying the electrical load of PMSG using DC/DC converter. For reduction of dynamic loads on VAWT during the transition from zone 2 to zone 3 and vice versa, the authors used a small transition zone, where the voltage U_{DC} is maintained at its maximum level.

In work [27] automatic control in zone 3 is held in the open-loop system—if the current in the DC link in excess of the acceptable value, the reference on the optimal angular velocity of VAWT decreases.

Thus, the development of effective control systems for small WECS with VAWT at large winds are still not sufficiently solved the problem. As shown in

Figs. 3 and 4 in power limitation modes, especially in the stall regulation, the control object is characterized by significant nonlinearity. Therefore, for the automatic control of VAWT in these modes is topical application of modern control methods of nonlinear systems.

3 Creation and Research of Power Limitation Systems of WECS by Classical Methods

General computer model of WECS has been developed in Matlab/Simulink environment to conduct research by computer simulation. It consists of the following subsystems: wind flow speed (test and turbulent), high-speed passive VAWT with aerodynamic characteristic (3), PMSG from SimPowerSystem library, AR operation imitator, in which transistors working with PWM have been replaced by controllable voltage sources for the purpose of faster simulation, PMSG optimal load control system, which works in accordance with principle (5). VAWT and PMSG parameters have been presented in the Appendix.

3.1 Development of Control Systems for Stall Regulation

Transition of WT in stall regulation mode is carried out by increasing VAWT load torque using PMSG. However, as shown in Fig. 3, VAWT angular velocity will decrease and its mechanical torque will also increase at wind speeds that are slightly higher than the nominal value for WT. With further increase of wind speed, VAWT torque will reach a maximum and then will start to fall because the operating WT point will move to decreasing area of $T_{WT}(\omega)$ characteristic. The analysis shows that for a generator pre-set load torque this area of the characteristic is statically unstable for WT operation. Stability can be achieved only by the automatic control in closed ACS.

Research studies conducted by computer simulation have shown that for stabilizing the operating VAWT point at a pre-set stabilizing power characteristic $P_{WT.n}$ (Fig. 4), the latter in such static unstable and nonlinear ACS cannot automatically adjust with required speed for the electric power, measured at the output of PMSG. It is necessary to carry out directly automatic adjustment of VAWT mechanical power. As it appears impossible to be measured, its value should be calculated, and it is not accurate computation, but the speed of obtaining at least an approximate value of P_{WT}. It can be easily done by the help of measured values of wind speed V and the generator angular velocity ω according to the expressions (1) and (3). On the structural scheme of developed ACS for stall regulation (Fig. 6) it is done by power estimator (PE). Obtained current value of the VAWT power $\hat{P}_{WT}$ at its output is compared with the nominal value $P_{WT.n}$. Their difference comes to power

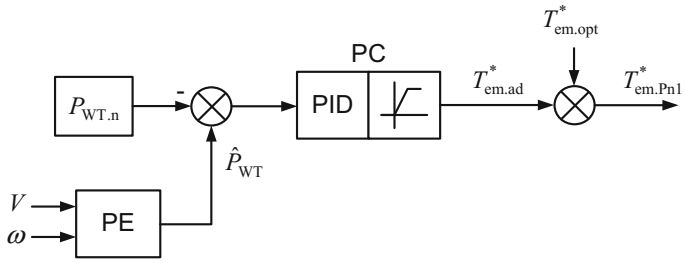

Fig. 6 Block diagram of the ACS, which provides passive stall regulation mode of VAWT

controller PC, which creates the reference for additional electromagnetic torque $T^*_{em.ad}$. It is added to the reference for electromagnetic torque $T^*_{em.opt}$ of PMSG formed by control system in case of partial-load of WECS.

Power limitation system works in the following way. In the partial-load mode of WECS $P_{WT} < P_{WT.n}$, that is why the output of the PC will be a negative signal, which is limited at 0. Therefore, the limitation system is not working. With increasing wind speed above nominal value there occurs condition $P_{WT} > P_{WT.n}$, which leads to the appearance of the reference $T^*_{em.ad}$ at the output of PC. It is added to $T^*_{em.opt}$, in resulting in forming a new reference $T^*_{em.Pn1}$ for electromagnetic torque, which will provide power limitation of VAWT on the nominal level with decreasing ω.

Mechanical power for simulations is limited at 1300 W. Power limitation system with PI and PID controllers has been researched. The best coefficients for these controllers as determined by computer simulation are as follows: PI controller—$k_p = 0.15$, $k_i = 0.10$; PID controller—$k_p = 0.75$, $k_i = 0.35$, $k_d = 1.10$.

Figure 7 shows the waveforms of computer simulation to illustrate the work of the power limitation system of VAWT by means of stall regulation. Test wind speed has been formed as follows (Fig. 7a): to 10 s $V = 9$ m/s, which is lower than the nominal, equal to 10 m/s, at 10 s wind speed is rapidly growing to 13 m/s, at 40 s it plummets to 11 m/s, and at 70 s goes back to 9 m/s. Thus, one can see the entry of WECS in power limitation mode and its exit from this mode. As a result of the formation of signal $T^*_{em.ad}$ at the PC output at high wind speeds there increases electromagnetic torque of PMSG (Fig. 7b) and the WT angular velocity decreases (Fig. 7c). This leads to the stabilization of VAWT mechanical power at a pre-set level of 1300 W (curves 1 and 2 in Fig. 7d), while in the case without limitation VAWT mechanical power increases significantly (curve 3 in Fig. 7d). Accordingly, the electric power at the output of WECS will also be limited at 750–850 W (curves

Fig. 7 Time dependencies of main coordinates of WECS, illustrating the entry and exit of it in ▶ power limitation mode by stall regulation: **a** test wind speed, **b** PMSG electromagnetic torque, **c** VAWT angular speed, **d** VAWT mechanical power, **f** electrical power at the output of WECS, **e** efficiency of PMSG, **g** linear armature current at phase of PMSG (*1*—PI controller, *2*—PID controller, *3*—without power limitation)

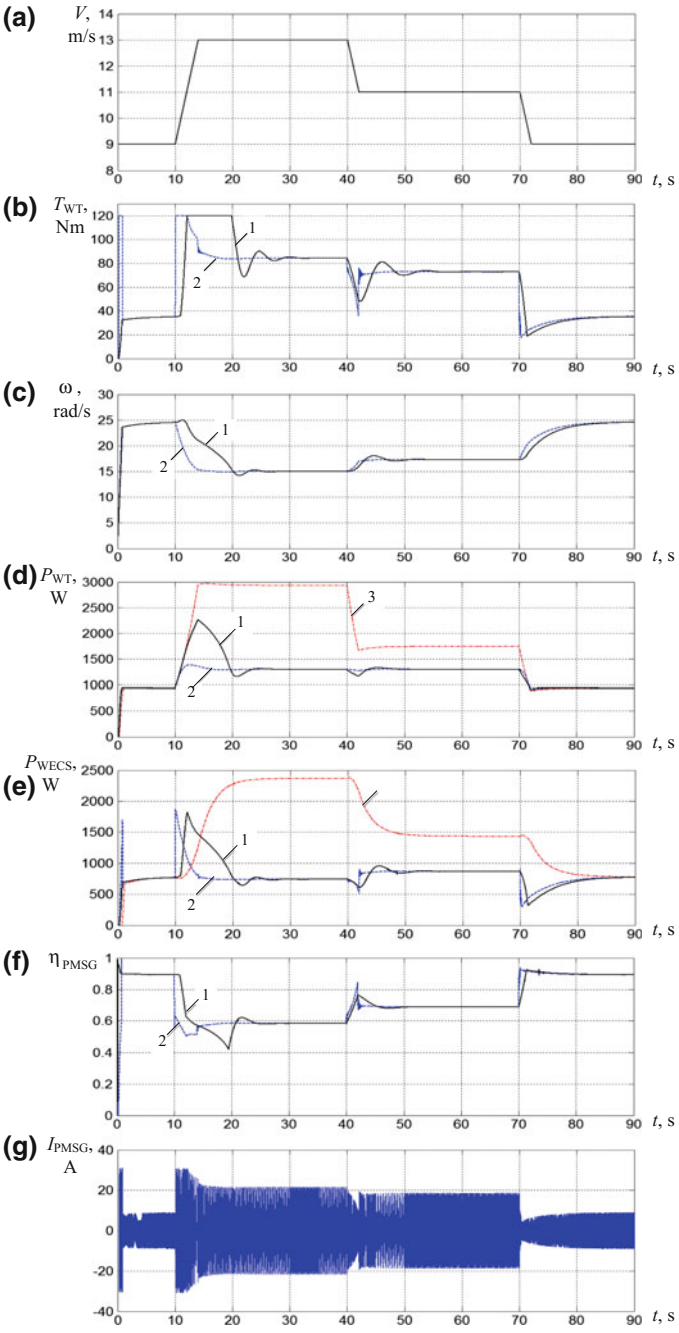
(a)
V, m/s
t, s
(b)
T_WT, Nm
1
2
t, s
(c)
ω, rad/s
1
2
t, s
(d)
P_WT, W
1
2
3
t, s
(e)
P_WECS, W
1
2
t, s
(f)
η_PMSG
1
2
t, s
(g)
I_PMSG, A
t, s

1 and 2 in Fig. 7e.), while without limitation it will increase to 2000 W (curve 3 in Fig. 7e). Decreasing the level of electrical power below the nominal one is due to the decrease in the efficiency of the generator η_{PMSG} (Fig. 7f) due to the growth of its electromagnetic torque and armature currents accordingly (Fig. 7g).

The obtained results of simulation have shown the different speed of regulation of power limitation systems of VAWT with PI and PID controllers. Unlike PI controller, PID controller enables the system to more quickly react to the increase in wind speeds above nominal value. This eliminates overshoot of VAWT mechanical power (Fig. 7d), due to the faster growth of PMSG electrical power (Fig. 7f), though. Thus, a system with PID controller has a less dynamic load on the mechanical part of WECS, and the system with the PI controller provides a less dynamic load on the electrical part. It is also possible to make settings of PID controller with compromising indices on mechanical and electrical parts of the WECS.

3.2 Development of Control Systems for Feathering Regulation

Transition of WT in feathering regulation operation mode is carried out by reducing the load torque of WT using PMSG. However, as shown in Fig. 2, the angular velocity of VAWT will be on the increase. Automatic control enables to easily stabilize VAWT mechanical power or output electrical power of WECS. Since the work of WT in this mode occurs on a stable area of its characteristics $T_{\text{WT}}(\omega)$, the possibility of automatic control is greatly enhanced compared to stall regulation.

The analysis shows that for reliable operation in strong wind it is essentially important to limit electrical power in PMSG output because it will not lead to its overheating and consequent failure. Mechanical overload in VAWT shaft can be permissible if they are projected in the construction of WECS. The same applies to the angular speed of both WT and the generator. Therefore, it is necessary to implement control system similar to stall regulation, with regulatory impact through electromagnetic torque of the generator in order to stabilize the output electrical power of WECS.

However, as confirmed by the research studies carried out by computer simulation, stabilization of the PMSG output power is difficult because of the unpredictable influence of electromagnetic torque: its increase is accomplished by increasing the armature current, resulting in lower output voltage because of losses in the windings. This can be accompanied by both increase and decrease in output power of the generator. To address this controversy, it has been decided to stabilize not the output power but electromagnetic power of PMSG instead, or the reference for this power, which is a bit easier.

All abovementioned solutions have been presented on the developed block diagram of the designed control system for feathering regulation (Fig. 8).

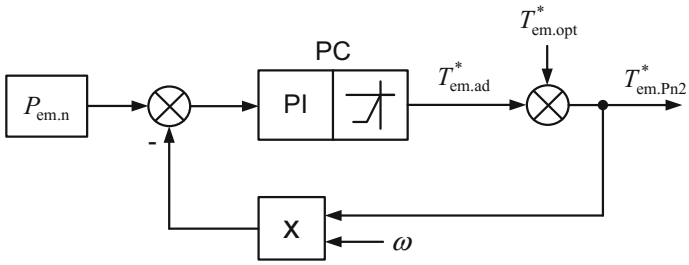

Fig. 8 Block diagram of the control system, which provides feathering regulation of VAWT

Power limitation system works in the following way. In the mode of partial-load of WECS electromagnetic power of wind turbine, P_{em} is lower than the nominal value $P_{em.n}$, because at the output of PC there will be zero signal provided by the limitation of PC. Thus, the power limitation system does not work. With increasing wind speed above nominal value there occurs condition $P_{em} > P_{em.n}$, which leads to the reference for additional negative electromagnetic torque $T^*_{em.ad}$, which reduces the value $T^*_{em.opt}$ at the output of the PC. It result in forming a new task for electromagnetic torque $T^*_{em.Pn2}$, which may provide limitation of the electromagnetic power of PMSG at nominal levels with increasing ω.

It is enough to use PI controller to limit pre-set electromagnetic power in this mode. $P_{em.n}$ is pre-set as the value of 1100 W, which provides electrical power limitation for WT at the level close to the nominal one. PI controller coefficients as determined by computer simulation are as follows: $k_p = 5.0$, $k_i = 2.0$.

Figure 9 shows the waveforms of computer simulation to illustrate the work of power limitation system of WECS by feathering regulation. Test wind speed (Fig. 9a) is the same as in the stall regulation. The output signal of the PC in power limitation modes provides the decrease of electromagnetic torque of PMSG (Fig. 9b) and the increase of VAWT angular velocity (Fig. 9c). This leads to the decrease in VAWT mechanical power (curve 1 in Fig. 9d) compared to the system without limiting power (curve 2 in Fig. 9d). Accordingly, the electric power at the output of WECS will be stabilized at 1050 W (curve 1 in Fig. 9e compared to curve 2 with no limitation). The efficiency of generator $\eta_{СГПМ}$ in this mode increases (Fig. 9f) because of its electromagnetic torque and armature current reduce, accordingly (Fig. 9g).

3.3 Comparative Analysis of VAWT Power Limitation Methods at High Wind Speed

The analysis of developed control systems structures and the results of simulation of WECS work on the test wind profile with the transition to high-speed wind and the return to slack wind have enabled to draw the following conclusions.

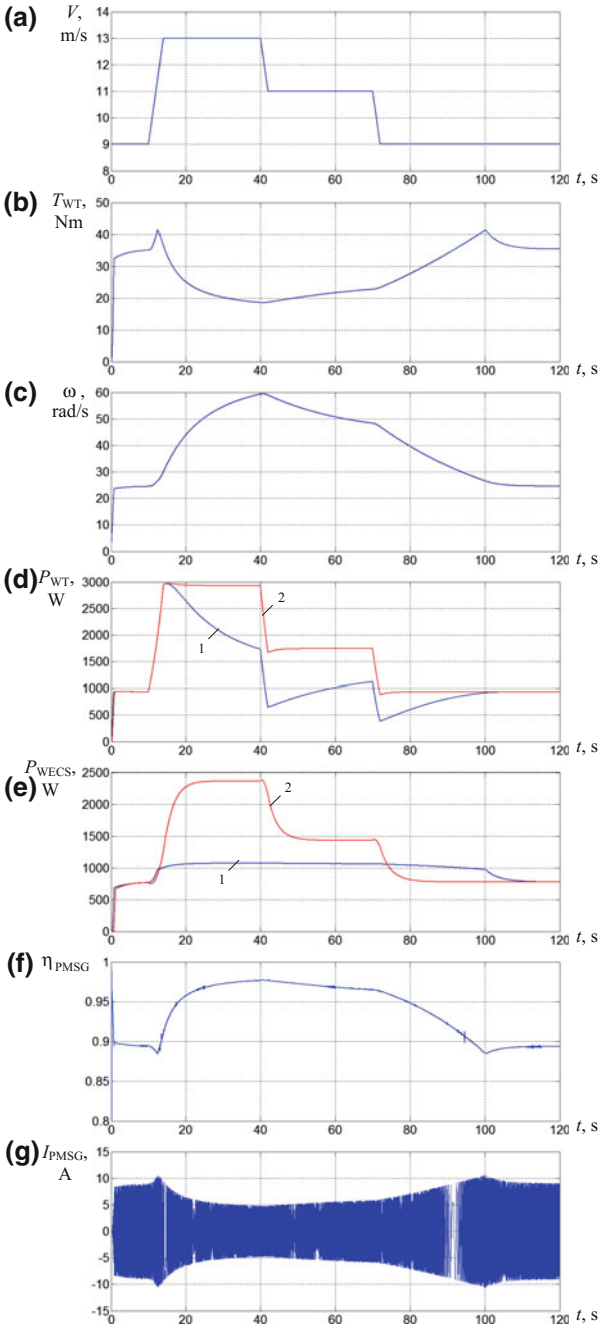
(a)
V, m/s
14
13
12
11
10
9
8
0
20
40
60
80
100
120
t, s
(b)
T_WT, Nm
50
40
30
20
10
0
(c)
ω, rad/s
60
50
40
30
20
10
0
(d)
P_WT, W
3000
2500
2000
1500
1000
500
1
2
(e)
P_WECS, W
2500
2000
1500
1000
500
(f)
η_PMSG
1
0.95
0.9
0.85
0.8
(g)
I_PMSG, A
15
10
5
0
-5
-10
-15

◂**Fig. 9** Time dependencies of main coordinates of WECS, illustrating the entry and exit of it in power limitation mode by feathering regulation: **a** test wind speed, **b** PMSG electromagnetic torque, **c** VAWT angular speed, **d** VAWT mechanical power, **f** electrical power at the output of WECS, **e** efficiency of PMSG, **g** linear armature current at phase of PMSG (*1*—with power limitation, *2*—without power limitation)

1. Stall regulation is characterized by a high degree of nonlinearity of the object related to the maximum of characteristics $T_{WT}(\omega)$, thus the satisfactory operation of the control system can be achieved only by VAWT mechanical power control, the value of which has to be calculated online using the measured approximate value of wind speed.
   Feathering regulation is characterized by significantly lower nonlinearity, which allows direct control of PMSG electromagnetic power and enables to build a simpler control system of this power.
2. The mechanical torque on the shaft of VAWT considerably increases in the stall regulation mode, but its angular velocity decreases, whereas in the feathering regulation mode, by contrast, mechanical torque decreases and the angular velocity increases. Therefore, implementation of such WECS power limitation modes requires different approaches to the design of mechanical parts of VAWT.
3. PMSG losses in copper are on the increase in the stall regulation mode as a result of a significant increase in electromagnetic torque, leading to a significant decrease in the efficiency of PMSG and, thus, electrical power at the output of WECS. By contrast, in feathering regulation mode losses in copper are reduced, although iron losses slightly increase because of increased frequency of electric move force, but they do not play a significant value in PMSG. This allows ensuring high value of generator efficiency in feathering regulation mode and to obtain more electric energy at the output of WECS in strong wind in comparison with the stall regulation.
4. Due to the direct control of PMSG electromagnetic power in feathering regulation mode its value can be stabilized at a pre-set nominal level regardless of changes in wind speed in the range of high speeds. Excess energy is going to accumulate as kinetic energy of the rotating parts of VAWT and PMSG, and then it will be eliminated by further nominal generator load. This provides much better smoothness of WECS generated electrical power in feathering regulation compared with the stall regulation.

The conducted analysis has shown a number of advantages of feathering regulation to limit the power of VAWT in high-speed wind operation. However, it eliminates one major drawback, i.e., a significant increase in VAWT angular velocity compared with the nominal one, which greatly complicates the design of VAWT and mechanical transmission and reduces the reliability of WECS. Therefore, further studies focus on improving stall regulation by applying new approaches to design ACS.

4 Fractional Order Control of Power Limitation of VAWT

4.1 Intelligent Methods of Electromechanical Systems Synthesis with the Use of Fractional Order Controllers

Nowadays it is evident that increasing the adequacy of traditional models, including electromechanical systems (EMS) units, is impossible by means of classical mathematics apparatus and approaches in integer order differential space. It is known that many physical phenomena, processes, and elements of EMS are described as dynamic systems by fractional order derivatives, i.e., they are characterized by fractality [28]. The perspective of applying fractional order derivatives (operators) and integrals in EMS is based on the following:

- the necessity to take into account peculiarities of fractality of EMS technological processes and elements in the creation of their models by using equations with fractional order derivatives or integrals;
- the advantages of fractional order controllers compared to classical ones in terms of robust control of fractal nature objects, as well as nonlinearity, multi-massive scale, backlash objects, etc.

A series of research studies has been devoted to the evaluation of fractality degree of natural phenomena that affect technological processes related to EMS functioning and their control objects in particular [29, 30]. Fractal phenomena include kinetic energy turbulence of air flows linked to wind fractal structure and changing temperatures of atmosphere layers [31], which is important for the WT operation. Their consideration has a significant impact on the "wind flow—wind wheel" model adequacy.

One way of solving the problem of dynamic stability and quality of power as generated by WT has been presented in [32]. Applied ACS implements the strategy of SMC using fractional order controllers in control loop by DC/DC converter. The system has significant advantages, viz. stability and robustness to parametric uncertainties of wind wheel and generator, as well as insensitivity to disturbances in the electrical network.

The synthesis results of various systems described by fractional order transfer functions (TF) have made it possible to obtain appropriate fractional order controllers. Reliable sources [33, 34] show much interest in fractional order PID controllers ($PI^{\nu}D^{\mu}$) with TF

$$W_{\mathrm{R}}(s) = K_{\mathrm{p}} + K_{\mathrm{i}} s^{-\nu} + K_{\mathrm{d}} s^{\mu}, \tag{6}$$

where K_{p}, K_{i}, K_{d} are the transfer coefficients under the proportional, integral and differential fractional components of the controller; ν and μ stand for fractional orders under integral and differential components of the controller.

The use of TF controller (6) is justified because its fractional integral and differential components provide more opportunities in the synthesis of ACS loops. Nevertheless, the search for $\left[K_p, K_i, K_d, \nu, \mu\right]$ vector to optimize synthesis results requires conducting the research in a 5-dimensional space. Thus, when using such controller structure it is necessary to set five parameters, i.e., two parameters more than in the case of conventional PID controller when $\nu = 1$ and $\mu = 1$. However, this extends the functionality of the controller in the process of optimizing EMS circuits compared to integer order controllers and therefore provides better flexibility in setting and quality of dynamic performance, which, accordingly, enables the solution to the problem of synthesis of EMS with more complex requirements, including robust synthesis.

EMS synthesis under the conditions of stability, quality, robustness, and insensitivity to disturbances with a certain frequency band requires a rational choice of fractional controller adjustment settings that allow taking into account the abovementioned conditions. The most effective approaches with the aim of finding optimal or suboptimal solutions to multi-dimensional purpose functions appear to be the intellectual methods, viz. Particle Swarm Optimization (PSO) and Genetic Algorithm (GA) as online methods which can be applied in the design of self-tuning systems.

For the purpose of parametric EMS optimization in the online mode an innovative approach has been offered which is based on the modification of two methods: the method of technological readjustment of closed systems [35], designed to detect required readjustment and calculate controller parameters by the reaction of closed EMS to pre-set disturbance, and the adaptive method with the use of EMS transition function [36]. The originality of the proposed approach lies in the application of the reference model of standard fractional order forms and intelligent methods. This method involves all kinds of transformations, including the ones with a preliminary definition of the model parameters as well as those with the direct transition from test transient process characteristics to optimal parameters adjustment. The required disturbance is introduced only into a closed system. The advantage of this approach can be obvious from the fact that it does not require to set EMS equipment in a special debug mode, which reduces its adjustment time.

The algorithm for selecting $PI^{\nu}D^{\mu}$ controller parameters to optimize a loop with a specific control object using PSO [37] and the transition function with the desired parameters is as follows.

1. The transition function with the desired parameters, pre-set time, sampling time and the number of calculation points is introduced into computer memory.
2. Five-dimensional swarm space (according to the number of varied controller parameters) for $PI^{\nu}D^{\mu}$ controller is built [37]).
3. At each iteration for each particle swarm element (the coordinate of controller parameters in 5-dimensional space) and its acquired parameters in the space motion, there is a transition function of the optimized loop which is compared

with the reference transition function in online mode. The particle whose parameters provide the lowest absolute standard deviation and lower than the previous iteration will be determined as the best one in this iteration, and its parameters will determine the trajectory of the other particles motion in the next iteration. The number of iterations can be set manually, or, alternatively, the procedure of iterative process termination can be introduced when the absolute standard deviation of the reference transition function from optimized loop transition functions is lower than the set one.

$PI^{\nu}D^{\mu}$ controller parameters search can be conducted with regard to the following typical transition functions points: time of the first achievement of 95% of transition default value t_{095}, the maximum deviation of the coordinate $y_{\max}$ or overshoot σ, time of achieving maximum deviation of the coordinate $t_{\max}$. According to the abovementioned algorithm, comparison of transition function with the reference one occurs only in certain specific points of the transition process, viz. t_{095}, $y_{\max}$ and $t_{\max}$.

4.2 Fractional Order Control of Stall Regulation of VAWT Power

The proposed method has enabled synthesis of control loop for WT power limitation in stall regulation mode, where instead of obtained (Sect. 3.1) PID controller

$$W_{PC}(\mathrm{s}) = 0.75 + 0.35s^{-1} + 1.1s^{1} \tag{7}$$

fractional order $PI^{\nu}D^{\mu}$ controller has been applied.

$PI^{\nu}D^{\mu}$ controller has been synthesized by the above-proposed approach by means of using specific points of fractional order transition function for $\omega_{oc} = 2$ c^{-1}: $t_{095} = 1.1$ s, $\sigma = 7.32\%$, $t_{\max} = 2.8$ s. The criterion for the completion of the synthesis is the achievement of the desired quality of the transition process with a pre-set standard deviation from the pre-set points of standard transition function. The optimization has resulted in obtaining fractional order controller with the following TF:

$$W_{PC}(\mathrm{s}) = 0.2 + 0.2s^{-0.9} + 1.0s^{0.5}. \tag{8}$$

Figure 10 shows basic waveforms of test wind speed reproduction with WT, similar to test wind speed shown in Fig. 7. Transition processes by means of using classical PID controller have been also displayed (7) for the purpose of comparison. It can be seen from the obtained results that the use of fractional order $PI^{\nu}D^{\mu}$ controller (8) makes it possible to slightly accelerate transition processes of entering WT power limitation mode and virtually eliminate their oscillation, which will have a positive impact on WT operation.

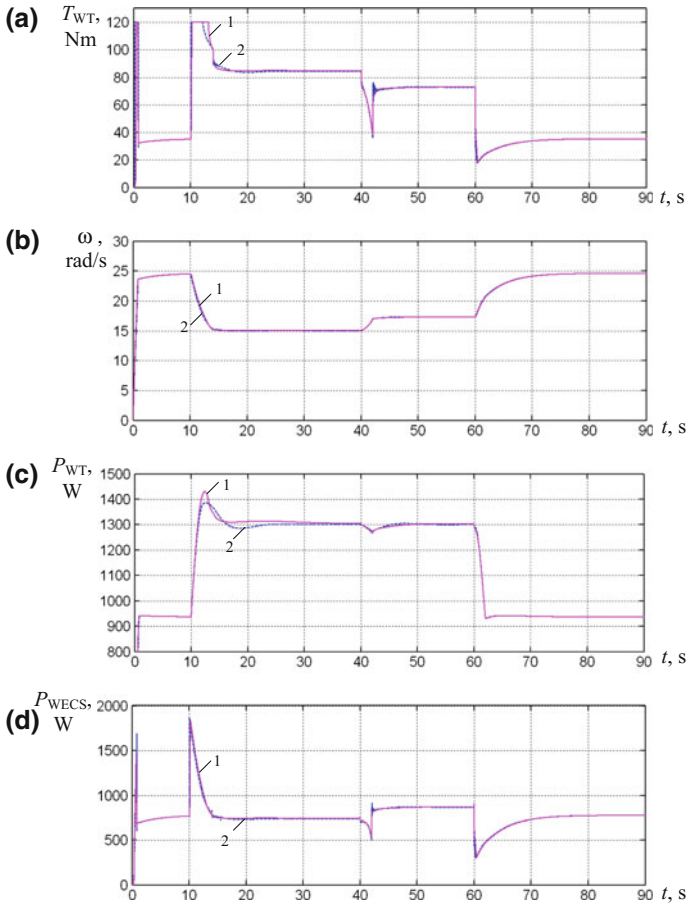

Fig. 10 Comparison of computer simulation results illustrating input and output of wind turbines in power limitation mode by stall regulation using conventional PID controller (curves 2) and fractional order $PI^{\gamma}D^{\mu}$ controller (curves 1): **a** PMSG electromagnetic torque, **b** VAWT angular velocity, **c** VAWT mechanical power, **d** output electrical power of WECS

5 Power Limitation of VAWT by Passive Stall Control in Energy-Shaping Control System (ESCS)

5.1 Energy-Shaping Control

Among the most promising methods of ACS synthesis of complex objects are those based on energy approaches [38], which allow design ESCS. Such energy-shaping control consists in the ACS assuring the passivity of the whole system. This allows

operating in the desired equilibrium point $\mathbf{x}_0$ since passivity itself provides oscillation damping in the system and its stable operation in the selected point [38].

In general, ESCS synthesis procedure consists in decomposing a system into simpler subsystems interlinked in some way [39], and finding such additional subsystems and interconnections that the total energy of the closed-loop system would attain a minimum in the equilibrium point $\mathbf{x}_0$ [40]. This equilibrium point is the control aim and is defined by the reference signal. In ESCS synthesis procedure both control object and ACS can be represented as an Euler–Lagrange system (ELs) [38] or the port-controlled Hamiltonian system (PCHs) [40]. System representation as PCHs makes it possible to consider the physical structure of the control object, which, in turn, greatly simplifies the part-differential equations to which the synthesis procedure is reduced; it also allows to simplify and make more transparent the stability analysis. PCHs model is as follows [40]:

$$\begin{cases} \dot{\mathbf{x}}(t) = [\mathbf{J}(\mathbf{x}) - \mathbf{R}(\mathbf{x})]\frac{\partial H}{\partial \mathbf{x}} + \mathbf{G}(\mathbf{x}) \cdot \mathbf{u}(t) \\ \mathbf{y}(t) = \mathbf{G}^{\mathrm{T}}(\mathbf{x})\frac{\partial H}{\partial \mathbf{x}} \end{cases}, \tag{9}$$

where $\mathbf{x}(t)$ is the state vector of the controlled system (the object), $\mathbf{J}(\mathbf{x}) = -\mathbf{J}^{\mathrm{T}}(\mathbf{x})$ is a skew-symmetric matrix which reflects the interconnection structure of the system, $\mathbf{R}(\mathbf{x}) = \mathbf{R}^{\mathrm{T}}(\mathbf{x}) \geq 0$ is a symmetric positive semi-definite matrix which reflects the dissipation in the system, $H(\mathbf{x}) = 0.5\ \mathbf{x}^{\mathrm{T}}\ \mathbf{D}^{-1}\ \mathbf{x}$ is the energy function of the controlled system, $\mathbf{D}$ is the diagonal matrix of inertias, $\mathbf{G}(\mathbf{x})$ is the port matrix, and $\mathbf{u}(t)$ and $\mathbf{y}(t)$ are vectors of input and output system energy variables.

According to [41], ESCS synthesis procedure is reduced to the writing of the mathematical model of the object in the PCHs form (9), the selection of a matrix of the control system ($\mathbf{J}_{\mathrm{a}}(\mathbf{x})$ and $\mathbf{R}_{\mathrm{a}}(\mathbf{x})$) and, thanks to the energy-shaping principles, interconnection and damping assignment, to the solving of the following matrix equation:

$$\begin{aligned} &[\mathbf{J}(\mathbf{x}) + \mathbf{J}_{\mathrm{a}}(\mathbf{x}) - (\mathbf{R}(\mathbf{x}) + \mathbf{R}_{\mathrm{a}}(\mathbf{x}))]\frac{\partial (H_{\mathrm{d}} - H)}{\partial \mathbf{x}} \\ &= [\mathbf{J}_{\mathrm{a}}(\mathbf{x}) - \mathbf{R}_{\mathrm{a}}(\mathbf{x})]\frac{\partial H}{\partial \mathbf{x}} + \mathbf{G}(\mathbf{x}) \cdot \mathbf{b}(\mathbf{x}) \end{aligned}, \tag{10}$$

where H_{d} is the desired energy function, which attain a minimum in the equilibrium point $x0$, and $\mathbf{b}(\mathbf{x}) = \mathbf{u}$ is the vector of input system energy variables, formed through feedback.

The results of synthesis are the elements of regulator matrix $\mathbf{J}_{\mathrm{a}}(\mathbf{x})$ that were found and the final equations of ESCS regulators [41–43]. However, during synthesis some elements of regulator matrices ($\mathbf{J}_{\mathrm{a}}(\mathbf{x})$ and $\mathbf{R}_{\mathrm{a}}(\mathbf{x})$) could be "free" [41–43], they are intended for ACS setting up and can be selected manually or calculated with parametrical synthesis procedure.

5.2 ESCS of WECS with VAWT

There already exist several variants of ACS of WECS, based on energy-shaping [24, 44–46]. In most cases, during the synthesis of ESCS of WECS authors consider the control object in simplified form—as a mechanical system. This approach is caused by the fact that electromagnetic time constants are much smaller than the mechanical ones, and that is why at mechanical systems ACS synthesis the inertia of the current circuit is usually not taken into account. However, in the WECS case, the current loop effect is quite important, as it should also provide a minimization of losses in the generator—in order to produce maximum WECS output power. That is why it's important to synthesize ESCS of WECS while taking into account electromagnetic part (Generator—Power converter—Load or Grid) [24]. Proposed in literature ESCS of WECS are synthesized for optimal power extraction mode and require additional adaptation for power limitation mode.

We synthesized ESCS of WECS while taking into account electromagnetic part (PMSG and power converter). PMSG is described in rotation coordinates d-q [47]. ESCS regulators, obtained by the described above approach, are as follows [24]:

$$\begin{cases} u_{\mathrm{dc}}\mu_d^* = -k\left(i_q - i_{q0}\right) + R_{\mathrm{s}} i_{d0} - pL_d i_{q0}(\omega - \omega_0) \\ \qquad\qquad - pL_q i_q \omega_0 \\ u_{\mathrm{dc}}\mu_q^* = k(i_d - i_{d0}) + R_{\mathrm{s}} i_{q0} + pL_q i_{d0}(\omega - \omega_0) \\ \qquad\qquad + p(\Phi + L_d i_d)\omega_0 \\ T_{\mathrm{em}}^* = T_{\mathrm{WT}} - r_3(\omega - \omega_0) \end{cases}, \tag{11}$$

where u_{dc} is a constant voltage in DC output circuit of power converter, μ_{d}^* and μ_{q}^* are the reference duty ratio functions in d-q frame, r_3 is the damping coefficients, which express mechanical damping of the control system, k is the decupling coefficient, which compensates the cross-links between d-axes and q-axes voltage control channels, i_{d} and i_{q} are d-axes and q-axes projections of the stator current vector, respectively, i_{d0} and i_{q0} are, respectively, d-axes and q-axes reference signals of the projections of current vector, L_d and L_q are d-axes and q-axes stator inductances, respectively, R_{s} is the stator resistance per phase, p is the number of rotor pole pairs, Φ is the rotor flux linkage, ω_0 is the reference VAWT speed, T_{em}^* is the signal of reference torque and TWT is the VAWT torque.

By correcting procedure of reference values forming [24] the expressions of new WECS of PMSG load without a wind speed sensor can be obtained:

$$\begin{cases} u_{\mathrm{dc}}\mu_d^* = -r_1(i_d - i_{d0}) - k\left(i_q - i_{q0}\right) + R_{\mathrm{s}} i_{d0} \\ \qquad\qquad - pL_d i_{q0}(\omega_{\mathrm{z}} - \omega_0) - pL_q i_q \omega_0 \\ u_{\mathrm{dc}}\mu_q^* = -r_2\left(i_q - i_{q0}\right) + k(i_d - i_{d0}) + R_{\mathrm{s}} i_{q0} \\ \qquad\qquad + pL_q i_{d0}(\omega_{\mathrm{z}} - \omega_0) + p(\Phi + L_d i_d)\omega_0 \\ T_{\mathrm{em}}^* = T_{\mathrm{WT}} - r_3(\omega_{\mathrm{z}} - \omega_0) \end{cases}, \tag{12}$$

where ω_z is the angular speed signal with delay.

In the obtained ACS (12) $\omega_z = \omega/(T_w s + 1)$, where T_w = 0.1 s is the time constant of TF in the feedback speed loop. The reference speed equals to current speed of WT $\omega_0 = \omega$. The reference current signal i_{q0} is known from the electromagnetic torque equation: $i_{q0} = 2/(3p) \cdot T^*_{em}/\left[\left(L_d - L_q\right) i_{d0} + \Phi\right]$, and the T_{WT} can be found like in OTC system [11] – $T_{WT} = K_T \omega^2$.

According to [24], ESCS with regulators (12) provides high static and dynamic performance of WECS without wind speed sensor, and also ensure the WECS operation in optimal response mode, which is meant to combine mechanical wind energy extraction by VAWT and electric energy losses in PMSG in such a way that the maximum of WECS output energy is obtained [24]. Such ESCS improves the WECS energy extraction, compared with the OTC, by 0.6–10% for different winds, WECS constructions, and ESCS settings. The maximum improvement of efficiency is ensured at turbulent winds with small average speed.

5.3 Power Limitation in ESCS

ESCS with regulators (12) are synthesized for optimal power extraction mode at partial-loading of WECS. In order to adapt it to operation in power limitation mode on high winds, we offer, depending on the operating mode, to change procedure of formation of the reference signal, in particular—speed ω_0 and torque T_{WT}.

Structural schema of adapted ESCS of WECS, with implemented possibility of stall regulation, is shown in Fig. 11. The system consists of four functional blocks.

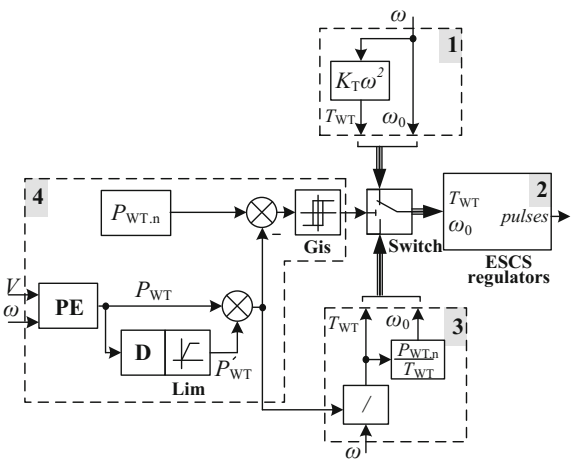

Fig. 11 ESCS of WECS adapted for power limitation mode

Block 1 forms reference signals by described in Sect. 5.2 method, and will take effect in optimal power extraction mode. Block 2 represents ESCS regulators (12). Block 3 forms objective signals in power limitation mode. Block 4 implements the logic function, which is responsible for switching between optimal power extraction and power limitation modes.

Proposed adapted ESCS works as follows. In Block 4 power estimator PE, based on wind speed V and angular speed ω signals, calculates the current value of mechanical power. This value is compared to PWT.n. The resulting difference ($P_{\text{WT.n}} - P_{\text{WT}}$) goes to hysteresis function Gis, which forms output «0» when $P_{\text{WT}} > 0.95\ P_{\text{WT.n}}$, and «1» when $P_{\text{WT}} < P_{\text{WT.n}}$ (hysteresis is introduced to avoid frequent switching in case $P_{\text{WT}} \sim P_{\text{WT.n}}$). Output signal of Gis controls switcher Switch, which conduct ESCS connection of reference signal former from Block 1 or Block 3.

In order to implement proactive control, similar to PID controller, in Block 4 a differential component D is introduced. It performs proactive control that reduces overshoot of mechanical power P_{WT}. This allows you to consider not only the current value of the mechanical power P_{WT} while controlling, but the dynamics of its change P'_{WT} as well. Then switching between modes will be based on the comparison result of $P_{\text{WT.n}} > P_{\text{WT}} + P'_{\text{WT}}$. Time constant of differential link is 0.1 s, and the value of the differential part P'_{WT} is limited on (0…0.25) $P_{\text{WT.n}}$.

If $P_{\text{WT}} + P'_{\text{WT}} > P_{\text{WT.n}}$, then ESCS switches to power limitation mode, and reference signals begin to form from Block 3. Based on the estimated value of mechanical power $P_{\text{WT}} + P'_{\text{WT}}$ and angular speed ω the new value of the mechanical moment TWT = PWT/ω is calculated and then goes to ESCS regulators as a reference signal of PMSM electromagnetic torque. The presence of the mechanical power differential part P'_{WT} in calculating of the reference torque signal accelerates system response to disturbances (an increase of wind speed V). Based on the calculated signal T_{WT} and the desired nominal mechanical power $P_{\text{WT.n}}$ desired reference speed signal $\omega_0 = P_{\text{WT.n}}/T_{\text{WT}}$ is being calculated. Such signals formation provides automatic movement of the system to the point of acceptable power extraction $P_{\text{WT.n}}$.

The comparative studies of the proposed adapted ESCS and OTC with stall regulation on PID power controller designed in Sect. 3.1 were conducted on the same test wind profile with the following ESCS settings: $k = -100$, $r_3 = 100$.

The research results (Fig. 12) show a slight increase in mechanical power overshoot for ESCS compared to OTC, but smaller transition process time and absence of oscillation, similar to the results obtained in Sect. 4.2 with the fractional order PID controller.

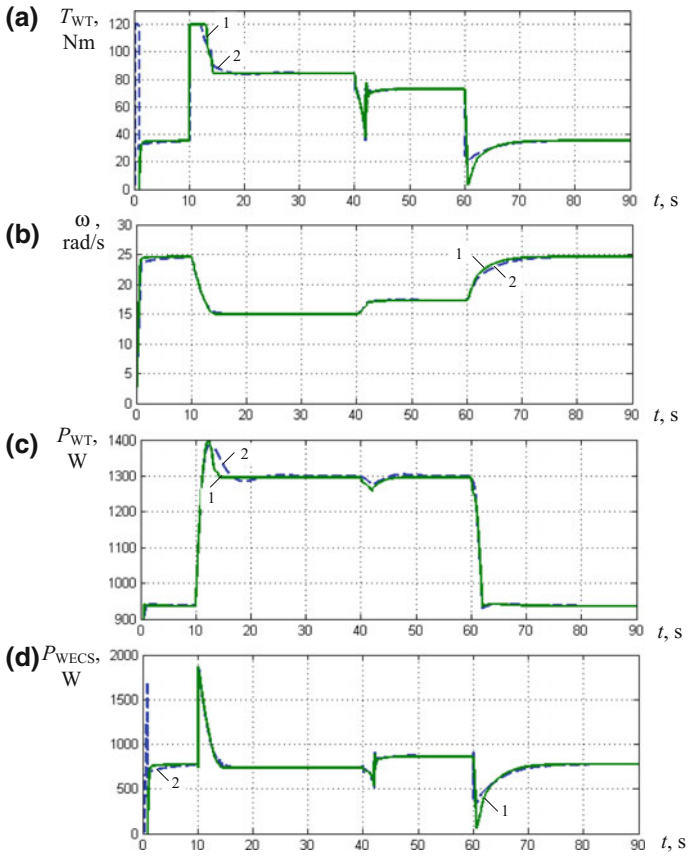

Fig. 12 Time dependencies of WECS operation with classical ACS (curve 2) and ESCS (curve 1): **a** PMSG electromagnetic torque, **b** VAWT angular velocity, **c** VAWT mechanical power, **d** electric power of WECS

6 Research of Developed System of VAWT Power Limitations in Turbulent Wind

To assess the effectiveness of the developed system of VAWT power limitation was held computer simulation research of WECS work at the wind with speeds close to real. For this used a computer model of turbulent wind, built on the Kaimal mathematical model [48]. The profile of average wind speed is set such that the instantaneous wind speed in certain intervals exceeds the rated value for research WECS of 10 m/s (Fig. 13a). The two control system's work was compared: the OTC with unlimited power and the OTS with power limitation through passive stall regulation with PID power controller. In the latter, an intermediate regarding the speed of regulation setting of power controller was applied—about halfway between PI and PID controllers studied in Sect. 3.1. To do this, the following coefficients of PID controller were applied: – $k_p = 0.35$, $k_i = 0.20$, $k_d = 0.30$.

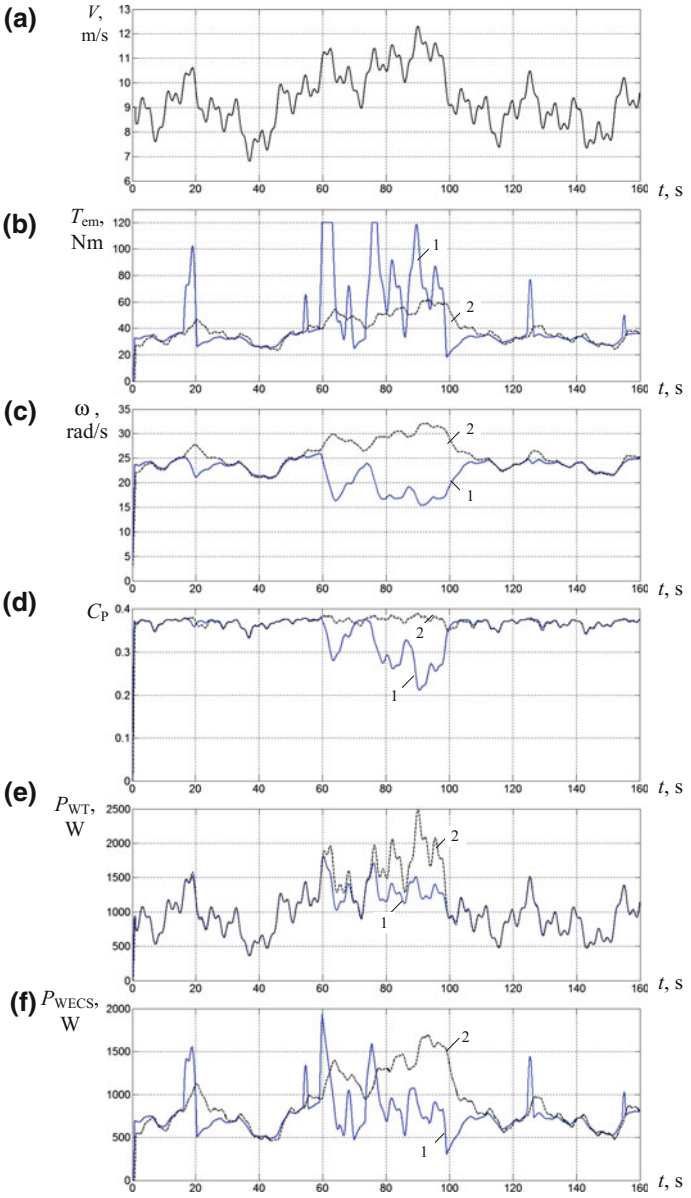

Fig. 13 Waveforms of main coordinates of WECS with different control systems at its work in turbulent wind: **a** wind speed, **b** PMSG electromagnetic torque, **c** VAWT angular velocity, **d** power coefficient, **e** VAWT mechanical power, **f** output electrical power of WECS (*1*—OTC with power limitation, *2*—OTC without power limitation)

The results of the simulation are shown in Fig. 13a–f. They demonstrate the effectiveness of developed control system of mechanical power limitation. In the intervals when the wind speed exceeds the nominal value—59…98 s (Fig. 13a), due to the formation of the maximum values of PMSG electromagnetic torque (Fig. 13b), VAWT angular velocity decreases (Fig. 13c). This leads to lowering of power coefficient C_P (Fig. 13d), in resulting the mechanical power of VAWT has reduced (Fig. 13e)—carried out a stall regulation. Average output electrical power of WECS also has reduced (Fig. 13f)—made its overload protection.

7 Conclusion

This article reports the results of a study by computer simulation of the work of WECS with SB-VAWT at the wind speeds greater than nominal in operating modes of power limitation by the passive stall and feathering regulation. To ensure the reliability of the mechanical parts of VAWT, preference is given to stall regulation, which is characterized by the nonlinearity of the control object. The article demonstrates different approaches to the development of the control system of power limitation modes: the use of classical PI and PID power controllers, PID controller of fractional order and the implementation of additional structures for ESCS. All developed control systems showed the effective limit of VAWT power during its work in turbulent winds at different speeds. The obtained results make it possible to choose an effective implementation of the control system of power limitation for various VAWT designs.

Appendix

(a) Parameters of the VAWT

WECS	VAWT					
$P_{WECS.n}$ (kW)	$P_{WT.n}$ (kW)	A (m^2)	r (m)	ω_n (rad/s)	$T_{WT.n}$ (N m)	J_Σ (kg m^2)
1.0	1.214	5.29	1.4	26.8	45.3	19.0

(b) Parameters of the PMSG

PMSG			
p	Φ, Wb	R, Ω	$L_d = L_q$,H
20	0.13	0.75	0.004

References

1. Harrison, R., Hau, E., Snel, H.: Large Wind Turbines: Design and Economics. Wiley, Chichester (2000)
2. Simic, Z., Havelka, J., Vrhovcak, M.: Small wind turbines—a unique segment of the wind power market. Renew. Energy **50**, 1027–1036 (2014)
3. Klymko, V.I.: Wind-solar systems for power supply of low power consumers (in Ukrainian). Ph.D. thesis, Lviv (2016)
4. Akello, P., Ochieng, F., Kamau, J.: Performance analysis of a direct drive permanent magnet generator for small wind energy applications. J. Sustain. Res. Eng. **1**(3), 1–9 (2014)
5. Bhutta, M., Hayat, N., Farooq, A., Ali, Z., Jamil, S., Hussain, Z.: Vertical axis wind turbine—a review of various configurations and design techniques. Renew. Sustain. Energy Rev. **16**, 1926–1939 (2012)
6. NACA profile coordinates—Airfoil tools. http://airfoiltools.com/airfoil/details?airfoil
7. Shchur, I.: Estimation of electromagnetic compatibility and efficiency of the adjustable load systems of PMSG in wind turbines. Przegląd Elektrotechniczny **1**, 85–90 (2011)
8. Stiebler, M.: Wind Energy Systems for Electric Power Generation. Springer, London (2008)
9. Alaimo, A., Esposito, A., Messineo, A., Orlando, C., Tumino, D.: 3D CFD analysis of a vertical axis wind turbine. Energies **8**, 3013–3033 (2015)
10. Tian-Pau, C., Feng-Jiao, L., Hong-His, K., Shih-Ping, C., Li-Chung, S., Shye-Chorng, K.: Comparative analysis on power curve models of wind turbine generator in estimating capacity factor. Energy **73**, 88–95 (2014)
11. Abdullah, M., Yatim, A., Tan, C., Saidur, R.: A review of maximum power point tracking algorithms for wind energy systems. Renew. Sustain. Energy Rev. **16**, 3220–3227 (2012)
12. Marimoto, S., Nakayama, H., Sanada, M.: Sensorless output maximization control for variable-speed wind generation system using IPMSG. IEEE Trans. Ind. Electron. **41**(1), 60–67 (2005)
13. Anders, G., Fredrik, B.: Robust VAWT control system evaluation by coupled aerodynamic and electrical simulations. Renew. Energy **59**, 193–201 (2013)
14. Sareni, B., Abdelli, A., Roboam, X., Tran, D.: Model simplification and optimization of a passive wind turbine generator. Renew. Energy **34**, 2640–2650 (2009)
15. Ming, C., Ying, Z.: The state of the art of wind energy conversion systems and technologies. Energy Convers. Manag. **88**, 332–347 (2014)
16. Shchur, I., Rusek, A., Klymko, V., Gastołek, A., Sosnowski, J.: Analysis of methods of electrical load of permanent magnet synchronous generator for small wind turbines. Maszyny Elektryczny, Zeszyty Problemowe **105**(1), 75–81 (2015)
17. Wang, Q., Chang, L.: An intelligent maximum power extraction algorithm for inverter-based variable speed wind turbine systems. IEEE Trans. Power Electron. **19**(5), 1242–1249 (2006)
18. Whei-Min, L., Chih-Ming, H.: Intelligent approach to maximum power point tracking control strategy for variable-speed wind turbine generation system. Energy **35**, 2440–2447 (2010)
19. Ying-Yi, H., Shiue-Der, L., Ching-Sheng, C.: MPPT for PM wind generator using gradient approximation. Energy Convers. Manag. **50**, 82–89 (2009)
20. Eftichios, K., Kostas, K.: Design of a maximum power tracking system for wind-energy-conversion applications. IEEE Trans. Ind. Electron. **2**, 486–494 (2006)
21. Iigo, K., Jon, A., Iigo, M., Jaime, J., Jos, I., Eider, R.: A novel adaptative maximum power point tracking algorithm for small wind turbines. Renew. Energy **63**, 785–796 (2014)
22. Brice, B., Tarek, A., Mohamed, E.: Sliding mode power control of variable-speed wind energy conversion systems. IEEE Trans. Energy Convers. **23**(2), 551–558 (2008)
23. Changliang, X., Qiang, G., Xin, G., Tingna, S., Zhanfeng, S.: Input–output feedback linearization and speed control of a surface permanent-magnet synchronous wind generator with the boost-chopper converter. IEEE Trans. Ind. Electron. **59**(9), 967–974 (2012)

24. Shchur, I., Rusek, A., Biletskyi, Y.: Energy-shaping optimal load control of PMSG in a stand-alone wind turbine as a port-controlled Hamiltonian system. Przegląd Elektrotechniczny **5**, 50–55 (2014)
25. Muteanu, I., Bratcu, A., Cutululis, N., Ceangă, E.: Optimal Control of Wind Energy Systems. Springer, London (2008)
26. Serban, I., Marinescu, C.: A sensorless control method for variable-speed small wind turbines. Renew. Energy **43**, 256–266 (2012)
27. Andriollo, M., De Bortoli, M., Martinelli, G., Morini, A., Tortella, A.: Control strategies for a VAWT driven PM synchronous generator. Int. Symp. Power Electron. Electrical Drives Autom. Motion SPEEDAM **2008**, 804–809 (2008)
28. Potspov, A.A., Chernykh, V.A.: Fractional calculation of A. Letnikova, fractal and scaling theory (in Russian). Phizmatlit, Moscow (2010)
29. Schafer, I., Kruger, K.: Modelling of lossy coils using fractional derivatives. J. Phys. D Appl. Phys. **41**, 1–8 (2008)
30. Freeborn, T., Maundy, B., Elwakil, A.: Fractional-order models of supercapacitors, batteries and fuel cells. Mater. Renew. Sustain. Energy **4**, 1–7 (2015)
31. Tijera, M., Maqueda, G., Yague, C., Cano, J.: Analysis of fractal dimension of the wind speed and its relationships with turbulent and stability parameters. In: Ouadfeul, S.-A. (eds.) Fractal Analysis and Chaos in Geosciences (2012). http://cdn.intechopen.com/pdfs/40877/InTech-
32. Vaikundaselvan, B.: Dynamic model of wind energy conversion systems with fractional order controllers for the variable-speed operation of wind turbine. Int. J. Eng. Sci. Adv. Technol. **2** (4), 1115–1121 (2012)
33. Asrom, K., Hagglund, T.: The future of PID control. Control Eng. Pract. **9**, 1163–1175 (2001)
34. Chen, Y., Moore, K.: Help working with abstracts relay feedback tuning of robust PID controllers with iso-damping property. IEEE Trans. Syst Man Cybernet. Part B (Cybernetics) **35**(1), 23–31 (2005)
35. Burceva, Y.S.: No searching method for calculating of controller settings on minimum quadratic criterion (in Russian). Ph.D. thesis, Moscow (2014)
36. Rotach, V.Y.: Automatic Control Theory. MEI, Moscow (2004). (in Russian)
37. Kopchak, B.L.: Approximation transition functions of fractional order polynomials (in Ukrainian). In: Odessa National Polytechnic University, Scientific and technical journal "Electrotekhichni ta compyuterni systemy" **14**, 20–27 (2014)
38. Ortega, R., van der Schaft, A., Mareels, I., Maschke, B.: Putting energy back in control. IEEE Control Syst. Mag. **21**(2), 18–33 (2001)
39. Ortega, R., van der Schaft, A., Escobar, G., Maschke, B.: Interconnection and damping assignment passivity-based control of port-controlled Hamiltonian systems. Automatica **38**, 585–596 (2002)
40. Ortega, R., van der Schaft, A., Castanos, F., Astolfi, A.: Control by interconnection and standard passivity-based control of port-Hamiltonian systems. IEEE Trans. Autom. Control **53**(11), 2527–2542 (2008)
41. Zou, Z., Yu, H., Tang, Y.: Maximum output power of PMSM based on energy-shaping and PWM control principle. In: IEEE International Conference on Automation and Logistics, Qingdao, China, pp. 1556–1560 (2008)
42. Li, J., Liu, Y., Wu, H., Chu, B.: Passivity-based robust control of permanent magnet synchronous motors. J. Comput. Inf. Syst. **12**(9), 4965–4972 (2013)
43. Tang, Y., Yu, H., Zou, Z.: Hamiltonian modeling and energy-shaping control of three-phase AC/DC voltage-source converters. In: IEEE International Conference on Automation and Logistics, Qingdao, China, pp. 591–595 (2008)
44. De Battista, H., Mantz, R., Christiansen, C.: Energy-based approach to the output feedback control of wind energy systems. Int. J. Control **76**(3), 299–308 (2003)
45. Wang, C., Zhou, J.: Hamiltonian control stabilization for grid-side converters in doubly-fed wind turbines. In: Chinese Automation Congress, Wuhan, China, pp. 1252–1257 (2015)

46. Pahlevani, M., Pan, S., Mash, J., Jain, P.: Port-Controlled Hamiltonian (PCH)-based control approach for wind energy conversion systems. In: IEEE 5th International Symposium on Power Electronics for Distributed Generation Systems, Wuhan, Galway, pp. 1–5 (2014)
47. Bose, B., Eisenhut, C., Krug, F.: Modern Power Electronics and AC Drives. Prentice-Hall, Upper Saddle River (2002)
48. Eisenhut, C., Krug, F.: Wind-turbine model for system simulations near cut-in wind speed. IEEE Trans. Energy Convers. **22**(2), 414–420 (2007)